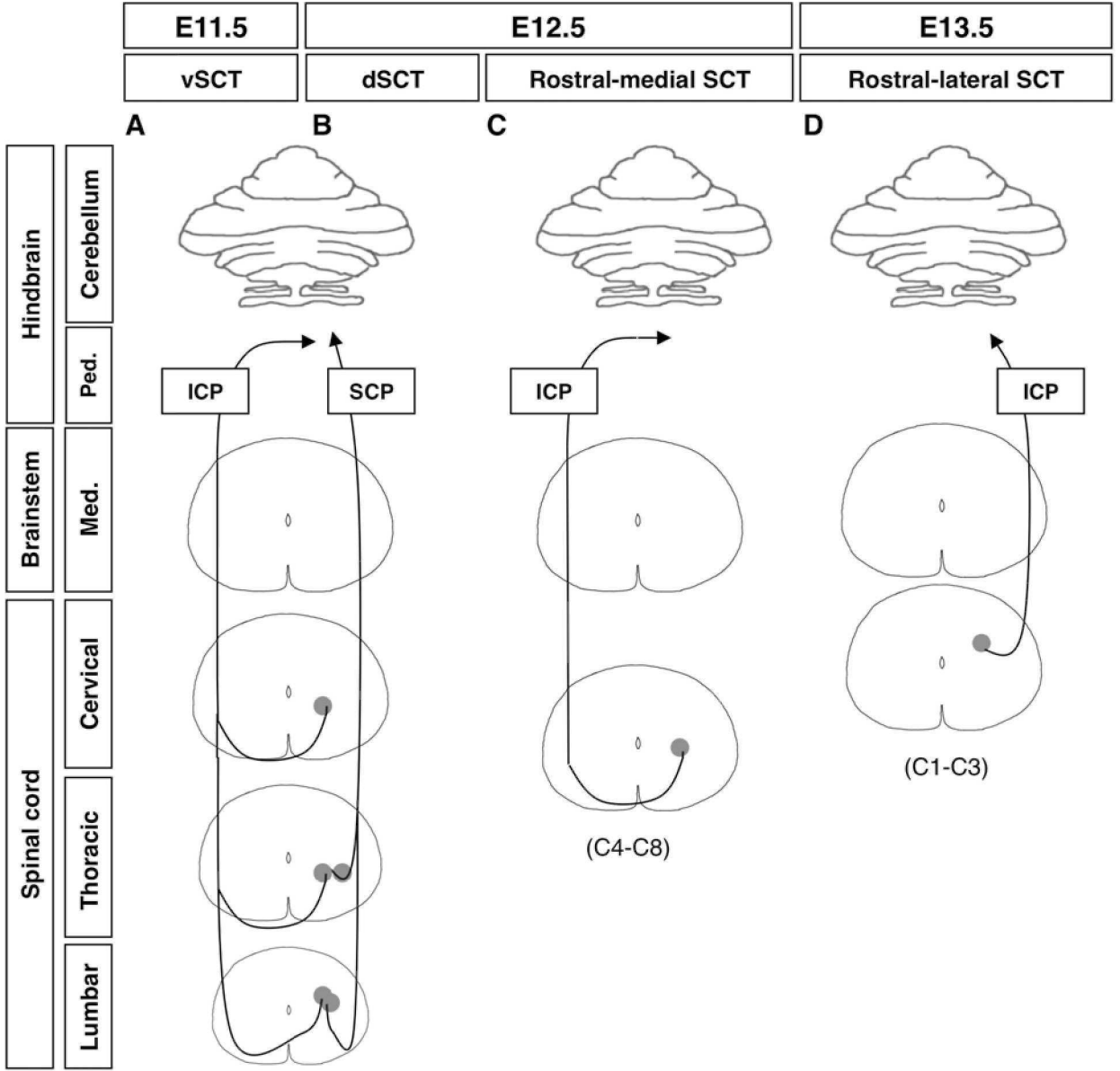
E11.5
E12.5
E13.5
vSCT
dSCT
Rostral-medial SCT
Rostral-lateral SCT
A
B
C
D
Hindbrain
Brainstem
Spinal cord
Cerebellum
Ped.
Med.
Cervical
Thoracic
Lumbar
ICP
SCP
ICP
ICP
(C4-C8)
(C1-C3)

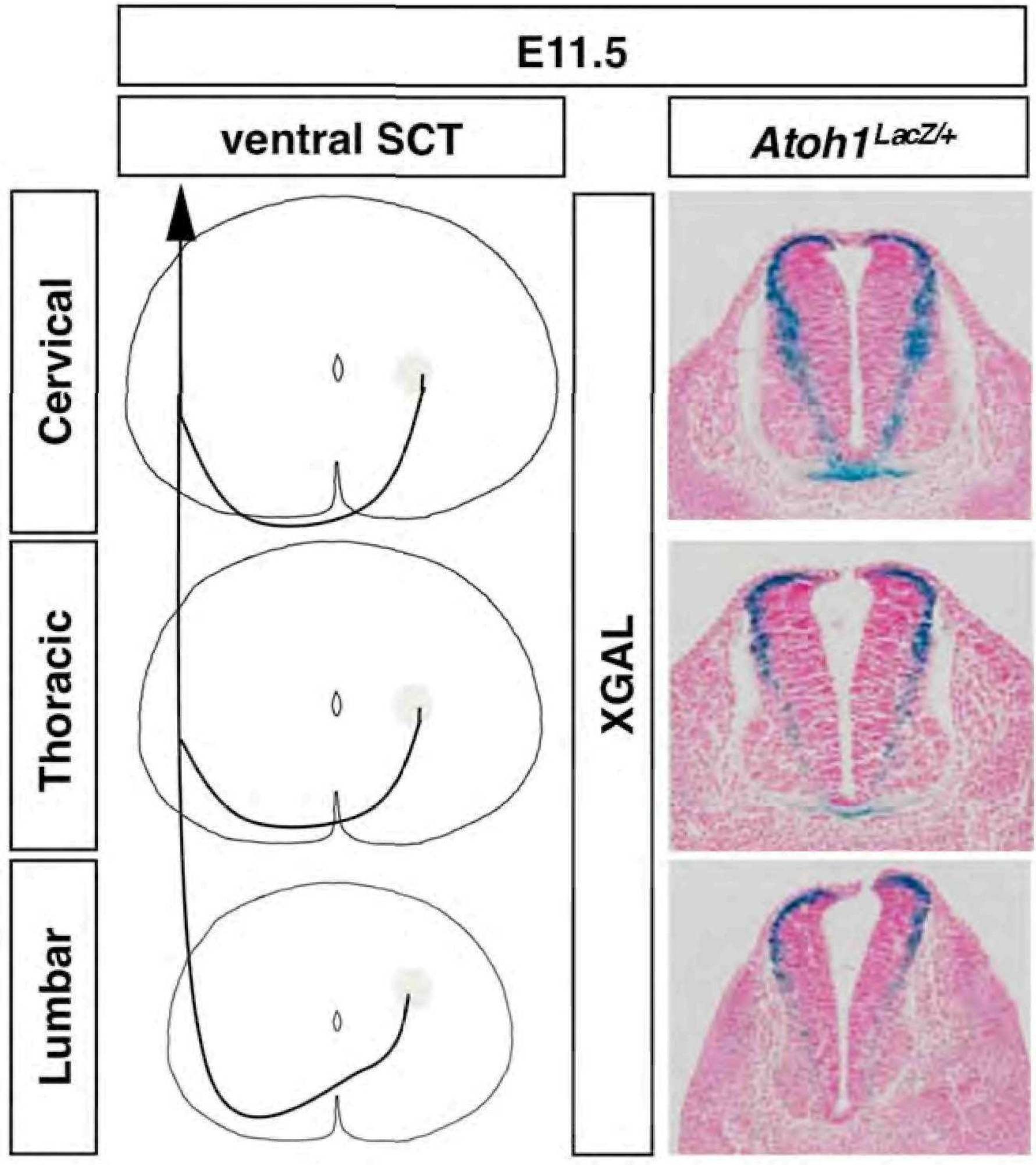
E11.5
ventral SCT
Atoh1LacZ/+
Cervical
Thoracic
Lumbar
XGAL

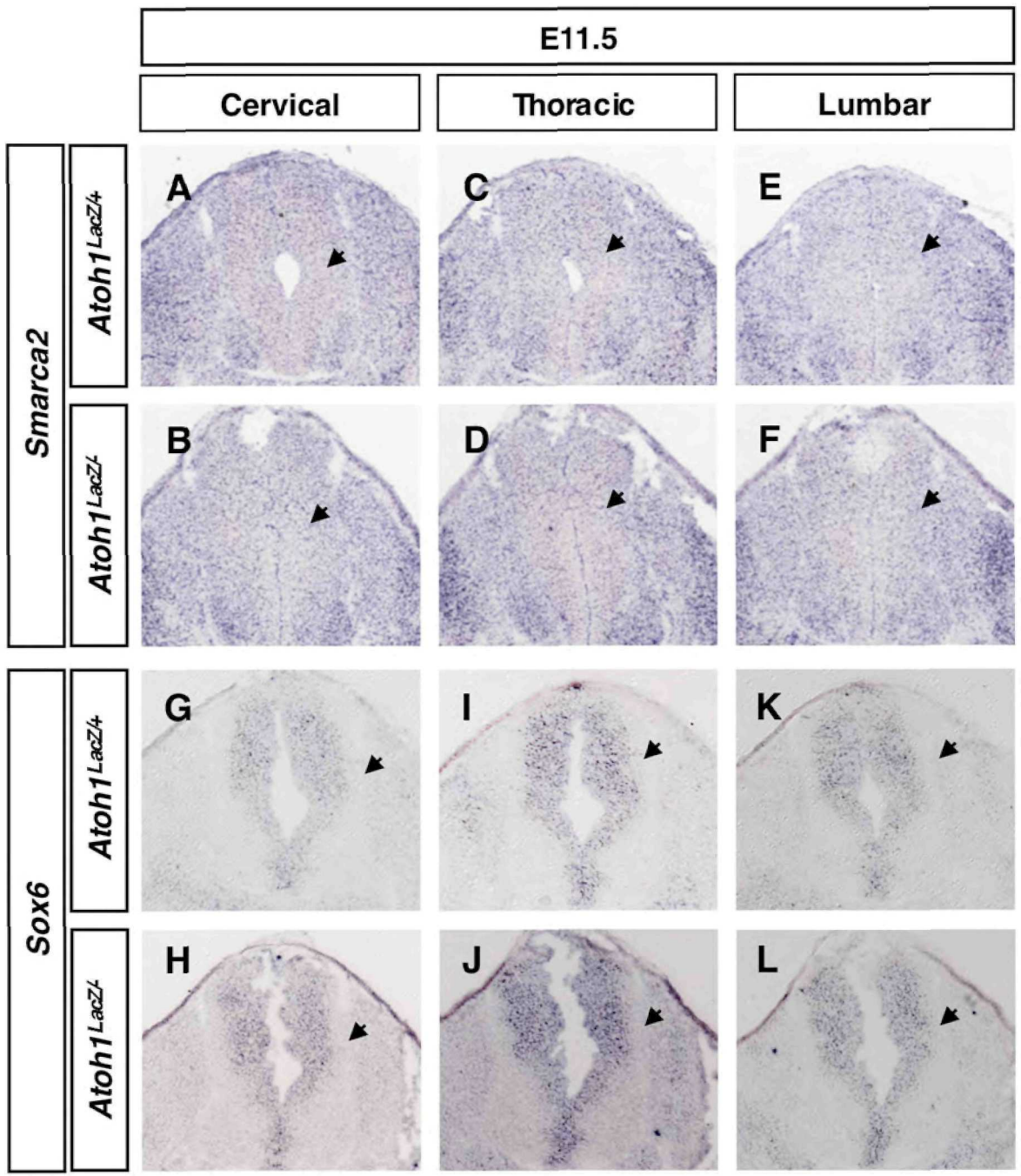
E11.5
Cervical
Thoracic
Lumbar
Smarca2
Atoh1LacZ/+
Atoh1LacZ/-
Sox6
Atoh1LacZ/+
Atoh1LacZ/-
A
B
C
D
E
F
G
H
I
J
K
L

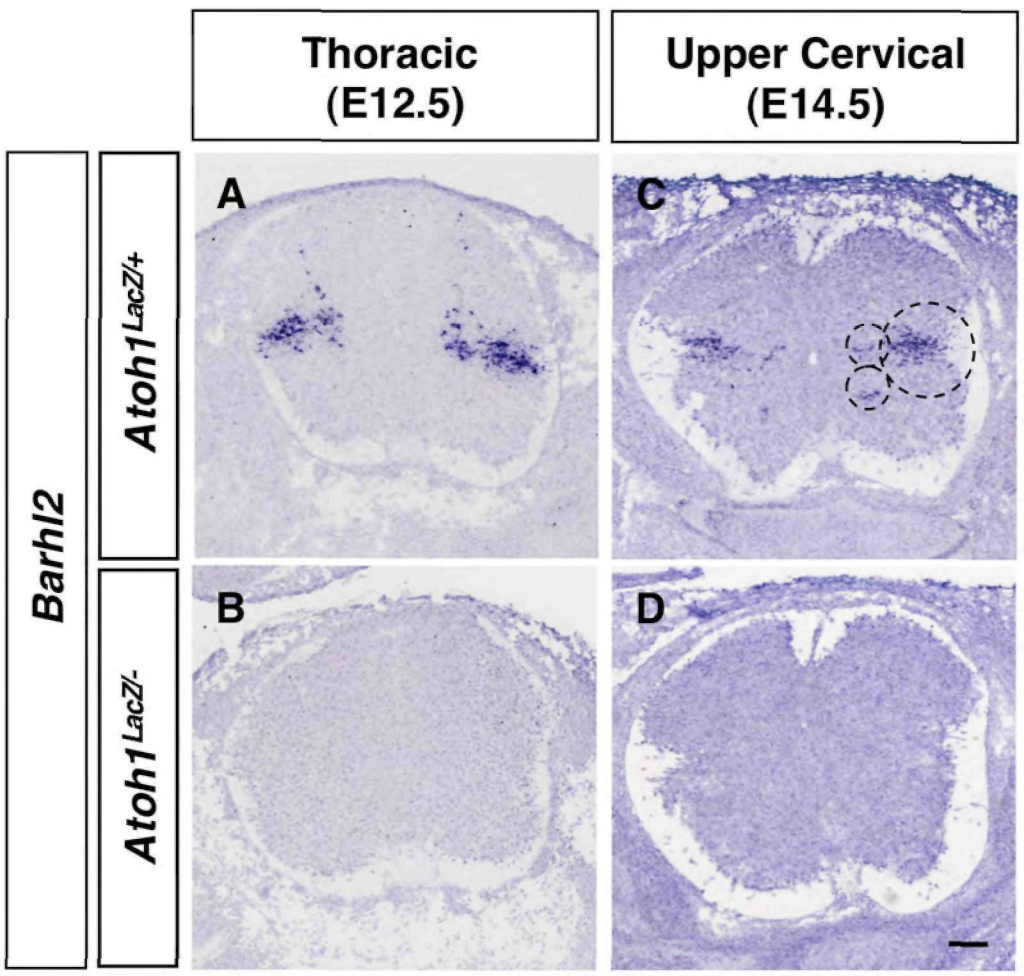
Thoracic
(E12.5)
Upper Cervical
(E14.5)
Barhl2
Atoh1LacZ/+
Atoh1LacZ/-
A
B
C
D

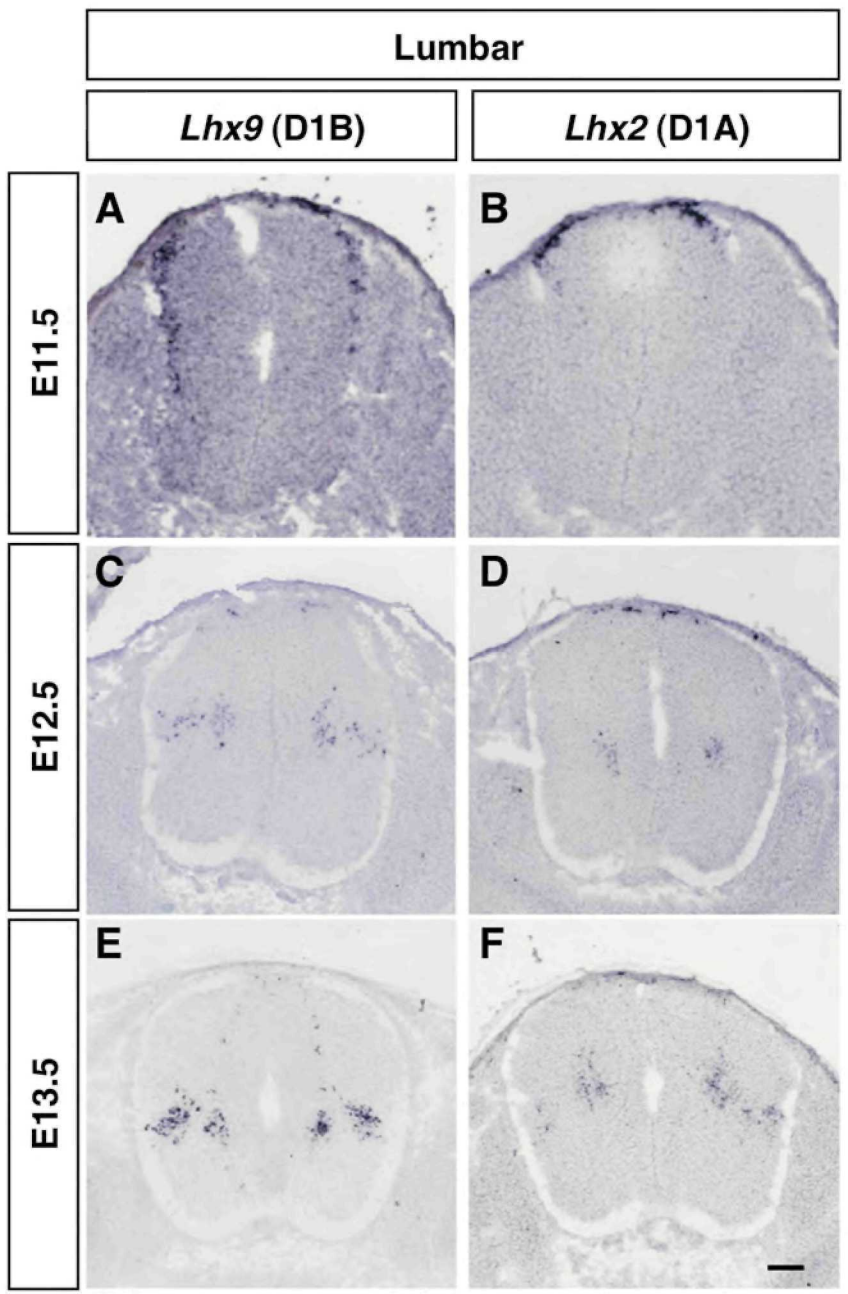
Lumbar
Lhx9 (D1B)
Lhx2 (D1A)
E11.5
E12.5
E13.5
A
B
C
D
E
F

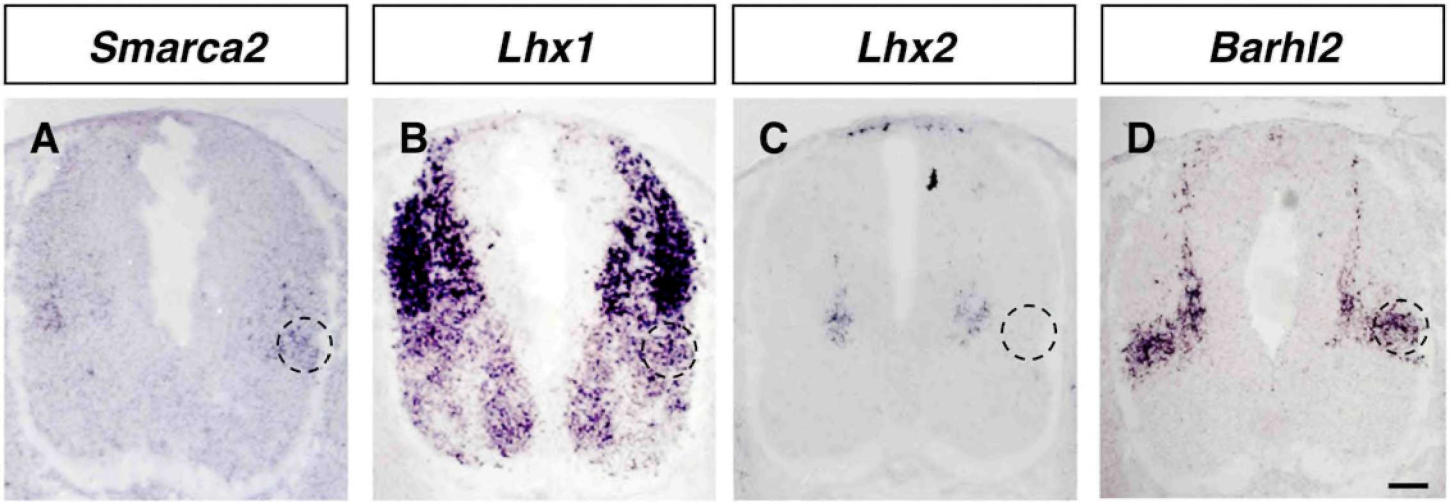
Smarca2
Lhx1
Lhx2
Barhl2
A
B
C
D

Fig. S1. Overview of the major subdivisions of the spinocerebellar tract. (A) The ventral spinocerebellar tract (vSCT) consists of contralateral projecting interneurons of the intermediate gray that reside along the length of the spinal cord and are established by E11.5. (B) On the other hand, the dorsal spinocerebellar tract (dSCT) ranges from forelimb to hindlimb and consists of ipsilaterally projecting interneurons of the intermediate gray that become evident by E12.5. (C) By E13.5, a rostral-medial tract, originally referred to as the rostral spinocerebellar tract (rSCT) resides at cervical levels and is made up of commissural interneurons located in or near the central cervical nucleus, whereas a previously unnamed rostral-lateral tract (D) is made up of ipsilateral interneurons in the central cervical nucleus, at upper cervical levels. All fiber tracts pass

through the superior (SCP) or inferior (ICP) cerebellar peduncles (Ped.) on their way to the granule cells and/or deep cerebellar nuclei. Reviewed in Tracey (1995).

Fig. S2. DP1-derived commissural interneurons comprise the ventral spinocerebellar tract. Xgal staining of *Atoh1*$^{LacZ/+}$ mice at E11.5 reveal contralaterally projecting cells in the intermediate gray at all spinal levels.

Fig. S3. *Smarca2* and *Sox6* are not expressed in interneuron populations at E11.5. In situ hybridization was performed on E11.5 mouse embryos. Shown are Cervical (A-B,G-H), Thoracic (C-D,I-J), and Lumbar (E-F,K-L). (A-F) RNA expression pattern of Smarca2 expression in wild type (A,C,E) and *Atoh1* null (B,D,F) embryos. At all levels of the spinal cord, staining is near background levels. (G-L) RNA expression pattern of *Sox6*. Expression is detected along the central canal of the spinal cord but not in areas corresponding to the migrating dorsal interneuron populations. Arrowheads denote the expected locations of cell bodies of DI1 derived cells at this time point.

Fig. S4. *Barhl2* is expressed in D1 derived cell types. In situ hybridization revealing the expression of *Barhl2* in *Atoh1*$^{LacZ/+}$ (A,C) and *Atoh1*$^{LacZ/-}$ (B,D) embryos. Expression is present at forelimb to hindlimb (A, E12.5 thoracic level shown) and upper cervical (C, dashed circles, E14.5 shown) levels and is identical to that of Xgal stained *Atoh1*$^{LacZ/+}$ embryos. (B,D) Expression of *Barhl2* is absent in *Atoh1* null animals. Scale bar 50 μm.

Fig. S5. *Lhx2* and *Lhx9* are expressed in medial and lateral DI1 interneurons. Wild type transverse sections using *Lhx9* (A,C,E) and *Lhx2* (B,D,F) specific riboprobes at lumbar levels. (A) At E11.5, *Lhx9*-expressing cells migrate away from the DP1 progenitor domain, whereas *Lhx2* expression remains at the dorsal aspect of the spinal cord. (C,E) *Lhx9* expression is equally distributed among medial and lateral clusters. However, *Lhx2* expression is first detected medially (D) then laterally (F). Scale bar 50 μm.

Fig. S6. *Lhx1, Smarca2* and *Barhl2* are expressed in the lateral DI1 interneurons, but not *Lhx2*. Adjacent sections of E12.5 wild type animals were subject to in situ hybridization using *Smarca2* (A), *Lhx1* (B), *Lhx2* (C) and *Barhl2* (D) specific riboprobes, respectively. At thoracic levels, the *Smarca2* subpopulation also expresses *Lhx1* and *Barhl2*, while it is *Lhx2* negative (black cycles).